Published in final edited form as:
J Stem Cell Transplant Biol. 2016 September 21; 2(1): . doi:10.19104/jorm.2017.109.

Xeno-Transplantation of macro-encapsulated islets and Pluripotent Stem Cell-Derived Pancreatic Progenitors without Immunosuppression

Michael A. Bukys[1], **Brandon Bakos**[1], **Solomon Afelik**[1], **Baruch Zimmerman**[2], **Barbara Barbaro**[3], **Dan Li Lin**[4], **Pilar Vaca**[3], **Tali Goldman**[2], **Avi Rotem**[2], **Margot Damaser**[1,4,5], **Jose Oberholzer**[3], **Uriel Barkai**[2], **Jan Jensen**[1]

[1]Department of Stem Cell Biology and Regenerative Medicine, LRI, Cleveland Clinic Foundation

[2]Beta-O2 Technologies, Rosh-HaAyin, Israel

[3]Division of Transplantation, Department of Surgery, University of Illinois at Chicago

[4]Advanced Platform Technology Center, Louis Stokes Cleveland VA Medical Center, Cleveland, OH

[5]Department of Biomedical Engineering, Lerner Research Institute, Cleveland Clinic

Abstract

Islet transplantation effectively treats diabetes but relies on immune suppression and is practically limited by the number of cadaveric islets available. An alternative cellular source is insulin-producing cells derived from pluripotent cell sources. Three animal cohorts were used in the current study to evaluate whether an oxygen-providing macro-encapsulation device, ‘βAIR’, could function in conjunction with human embryonic stem cells (hESCs) and their derivatives. The first cohort received macro-encapsulated undifferentiated hESCs, a second cohort received hESCs differentiated to a pancreatic progenitor state with limited endocrine differentiation. A reference cohort received human islets. Macro-encapsulation devices were implanted subcutaneously and monitored for up to 4 months. Undifferentiated pluripotent stem cells did not form teratoma but underwent cell death following implantation. Human C-peptide (hC- peptide) was detectable in host serum one week after implantation for both other cohorts. hC-peptide levels decreasing over time but remained detectable up to the end of the study. Key factors associated with mature endocrine cells were observed in grafts recovered from cohorts containing islets and hESC-derivatives including C-peptide, insulin, glucagon and urocortin 3. We conclude that the ‘βAIR’ macroencapsulation device is compatible with both human islets and pluripotent derivatives, but has a limited capability of sustaining undifferentiated pluripotent cells.

Keywords

cell therapy; encapsulation; oxygen; insulin; islet transplantation; pluripotent

Lead Contact: Jan Jensen, Ph.D, Asso. Prof., Department of Stem Cell Biology and Regenerative Medicine, Lerner Research Institute, Cleveland Clinic Foundation, 9500 Euclid Ave, Cleveland, OH, 44195, USA, jensenj2@ccf.org, Phone: + 001 216 445 0990

Introduction

Islet transplantation is an effective treatment for type I diabetes ([1,2] and http://www.citregistry.org/). However, patient demand for islets of Langerhans far exceeds the numbers available for transplantation, severely limiting this treatment option. Human embryonic stem cells (hESC) are a promising alternative source of insulin secreting cells. hESCs have an unlimited growth potential and the capacity to differentiate to any cell-type of the body [3]. Combined, these qualities imply the possibility of a limitless source of insulin producing beta-cells. However, two caveats to the use of hESC are the autoimmune rejection of implanted biologic material and the possibility of teratoma formation [4]; the latter risk is further enhanced if co-administering immunosuppressive drugs.

Considerable advancements in differentiating pluripotent cultures into functional pancreatic endocrine cells have occurred over the last decade [5,6,7,8,9,10], and normoglycemic restoration in diabetic mice through the implantation of such cells has been demonstrated [6,8,9,11,12] The best-known approach, pioneered by Kroon et al. [6], relies on implantation of pancreatic progenitors in a protective sac which in turn differentiate *in vivo* to form mature functional endocrine cells by an as yet poorly understood mechanism [8,13,14] The *in vivo* maturation process generally takes 2–3 months, and preclinical testing demands the use of immuno-compromised animals. Oxygen-replenishment macroencapsulation technology in conjunction with pluripotent derivatives has not been addressed at present. Generally, evaluation of encapsulation technologies have been performed using human islets (reviewed in [15]).

‘βAIR’ is an immuno-protective macro-encapsulation device previously shown to restrict the influx of host immune molecules and cells while permitting small molecule transfer (glucose, nutrients) and endocrine communication (e.g insulin) between graft and host [16,17] The ‘βAIR’ macro-encapsulation device contains a refillable air reservoir and provides a protective shielding for endocrine material through a dual-layer polytetrafluoroethylene (PTFE) membrane. Device functional testing has been performed in rats [18], pigs [19], and human [17] Demonstrating iso- and allo-type immunoprotection, rat islets encapsulated in ‘βAIR’ were capable of restoring normoglycemia in streptozotocin (STZ) induced diabetic rats [19,20]. Implanted devices sustained islets within a rat host for three months, and the host tissue immediately adjacent to the implantation site became vascularized. Gottingen minipigs were implanted with xenogeneic (rat) islets demonstrating the device’s ability to xenoprotect grafts from the host immune system [19] Importantly, glucose stimulated insulin secretion of pre-implantation islets was equivalent to the retrieved post-implantation material. More recently, a clinical study demonstrated that the ‘βAIR’ encapsulation technology is capable of sustaining islet viability and endocrine function for up to 10 months [17]. In the current study, we evaluate the ‘βAIR’ technology ability to safely accommodate and sustain hESC-derivatives within an immuno-competent rodent host, thus providing a safe method of implanting hESC derivatives without the need for immunosuppression.

Materials and Methods

Animal usage and procedures

All of the work performed was IACUC approved and detailed in protocol 2011–0628. In an effort to randomize the results outbred female Lewis rats were matched for weight and age (8w old, 190 – 216 grams (Jackson Laboratory Bar Harbor, ME)). Devices were refueled daily with a gas mixture composed of 55% nitrogen, 40% oxygen and 5% carbon dioxide (Praxair Danbury, CT special order). Rats were anesthetized using an isoflurane chamber before washing the skin covering refueling ports with ethanol. A 27 gauge needle (BD Biosciences San Jose, CA #305109) was inserted into the each of the two ports. A filtered (Millipore Allen, TX #SLFG025LS) syringe (BD Biosciences San Jose, CA 302832) containing gas mixture was affixed to one of the needles (side switched daily), while the other served as an exhaust to displace used gas. Rats were bled through the tail vein bi-weekly for blood collection.

Four months after the initial implantation streptozotocin (STZ) (MP Biomedical Solon, OH #02100557) was reconstituted to a final concentration of 7.5mg/ml in a 110mM sodium citrate buffer immediately before use. Rats were anesthetized in an isoflurane chamber, weighed and subjected to an intraperitoneal injection of 50mg STZ per kg of weight. Daily weights and blood glucose measurements were taken using an OneTouch Ultra glucometer (LifeScan Inc Milpitas, CA). After 3 days Linplant Sustained Release Insulin Implants (Linshin Canada, Toronto, Ontario #LHR-10BV) were inserted subcutaneously in the upper abdominal region using a 12G trocar. Daily measurements of weights and blood glucose levels continued for an additional week until all remaining rats were euthanized.

Trial cohorts

Three cellular groups were used for implantation within this trial (outlined in Fig 3A–B). The first group (undifferentiated hESCs) was a negative control. The second group (hESC derived pancreatic progenitors) was designed to evaluate the safety of the ‘βAIR’ device in conjunction with pluripotent derivatives. The third group (human islets) independently assessed the ability of the ‘βAIR’ device to sustain functional islets and served as a reference for the two hESC derived groups. Devices were inserted subcutaneously along the left flank of the rats with the air ports anterior positioned behind the neck.

Cell culture maintenance and differentiation

The human embryonic stem cell line WA01 (H1) was maintained through co-culture with irradiated mouse embryonic feeders. Pluripotent cells were passaged onto growth-factor depleted Matrigel (BD Biosciences San Jose, CA #354230) followed by 3 days of growth before initiating differentiation. A stage-wise description of the differentiation protocol used is outlined in Fig. 1A. Stage 1 consisted of a 3-day incubation in RPMI containing 2% albumin (Sigma-Aldrich St Louis, MO #A8806), 100ng/ml Activin A (Peprotech, Rocky Hill, NJ #120–14), 8ng/ml bFGF (Life Technologies Carlsbad, CA #13256029) and 20ng/ml Wnt3a (R&D Minneapolis, MN #5036-WN/CF). Wnt3a was only applied on the first day of stage 1, aiding the formation of definitive endodermal cells. Stage 2 consisted of an 8-day incubation in DMEM/F12 containing 2μM retinoic acid (Sigma-Aldrich St. Louis, MO

#R2625), 100ng/ml Noggin (R&D Minneapolis, MO #3344-NG), 250nM cyclopamine (Calbiochem San Diego, CA #239804), 100ng/ml Fgf10 (Peprotech Rocky Hill, NJ #100–26) and 1% Hyclone defined FBS (Thermo Scientific Waltham, MA #SH300700,02) for the first four days and 1% B27 (Life Technologies Carlsbad, CA #08–00855A) for the following four days. Stage 3 consisted of a 3-day incubation in DMEM/F12 containing 2μM retinoic acid, 100ng/ml Noggin, 250nM cyclopamine, 20ng/ml Wnt3a, 50ng/ml Activin A and 1% B27. Stage 4 consisted of a 12 day incubation in DMEM/F12 with 12mM Glucose supplemented with 50μM DAPT (Sigma-Aldrich St. Louis, MO #D5942), 0.5μM 1,25 (OH)2 Vitamin D3 (EMD Chemical Billerica, MA #679101), 1μM ALK5 inhibitor (EMD Chemical Billerica, MA #616452), 1mM Sodium Propionate (Sigma-Aldrich St. Louis, MO #P1880) and 50 μM 8-Br-cAMP (Sigma-Aldrich St. Louis #B7880). Implant preparation for the hESC derived groups was accomplished by treating differentiated cell cultures with collagenase for five minutes at which time cells were detached from flasks by gentle pipetting. Cells were then pooled and an aliquot was treated with trypsin to estimate cell number. Cultures were grown overnight in suspension as cellular aggregates before being loading into macroencapsulation devices. Aliquots from each respective stage and the overnight culture were taken for RNA isolation and IHC analysis.

Islet Purification:

Human islet preparations were obtained from the islet isolation program at the University of Illinois at Chicago. The isolation, purification, and culture procedures were performed as previously described [2,21,22] Briefly, the pancreata were trimmed and distended with collagenase and digested using a modified Ricordi semiautomatic method [21,22] The digestion phase was stopped between 10–20 minutes based on microscopic observation of islet cleavage (degree of islets releases from exocrine tissue) and tissue volume by the same experienced personnel. Digested tissue was then purified in a continuous density gradient using the UIC-UB gradient [23] in a Cobe 2991 cell separator (Cobe 2991, Cobe, CO) and subsequently cultured and maintained in CMRL 1066 culture media (Corning Corning, NY #99–785-CV) at 37°C supplemented with 2.5% Human Serum Albumin (Grifols NDC Los Angeles, CA #68516–5216-2), 0.244% Sodium Carbonate (Hospira Lake Forest, IL #0409–6625-02), 10mM HEPES (Mediatech-Cellgro Manassas, VA #25–060-CI), Ciprofloxacin (Hospira Lake Forest, IL #0409–4778-86) and 0.2% Insulin- Transferrin-Selenium (Invitrogen Carlsbad, CA #41400–045). The medium was changed every other day following centrifugation of islets at 300 RPM for 5 minutes.

Loading of devices and implantation surgeries

Cohorts 1 received undifferentiated hESCs, cohort 2 received differentiated hESCs and cohort 3 received human islets. ‘βAIR’ devices were loaded by mixing 3×10^6 cells (3000 islets for group 3) from the respective groups with a 2.5% high guluronic acid alginate (G=0.68) solution. This mixture was stirred to assure equal distribution of the biomass followed by distribution onto devices. Devices were then incubated for 16 minute in a Strontium solution (70 mM $SrCl_2$, 12.5 mM NaCl, 20 mM Hepes pH 7.4) to establish cross-linking of the alginate. Excess Strontium solution was washed off the alginate/cell slab. After the respective different cellular groups were seeded in an alginate slab the face of ‘βAIR’ devices was subsequently covered by a semi-permeable bi-layered PTFE membrane

(Millipore Allen, TX #SLGSM33SS). Silicone glue attached the Biopore membrane over the alginate slab and was secured further to the device using an O-ring. Devices were implanted subcutaneously on the left of the upper abdominal flank with two 7 cm polyurethane tubes connected to the refueling air-ports positioned at the upper back. Sutures were removed between 5–7 days post-surgery with no additional post-surgery care needed.

ELISA analysis

Centrifugation was used to clear cellular components from blood samples. Samples were analyzed on ultrasensitive C-peptide ELISA test kits (Mercodia Uppsala, Sweden #10–1141-01) using manufacturer's specifications. Standard curves and best fit lines were generated using Prism graphing software. Assaying rat serum for antibodies against human C-peptide (hC-peptide) was performed by incubating equal volumes of human and Rat serum at ambient temperature for 1 hour. Mixed serum samples were then subjected to 10% by volume Protein A/G PLUS-agarose beads (Santa Cruz Dallas, TX #sc-2003). Overnight incubation at 4°C on a Labnet Mini Labroller was followed by centrifugation at 2500RPM to clear Protein A/G PLUS-agarose beads. Supernatant was analyzed by ELISA on Ultrasensitive C-peptide ELISA (Mercodia Uppsala Sweden, #10–1141-01) at a 1/4 dilution.

RNA and immunohistochemistry analysis

RNA extractions of all bio-material used throughout the trial was performed using TRIzol (Life Technologies Carlsbad, CA). Reverse transcription of RNA samples was performed using the reaction conditions provided with qScriptTM cDNA SuperMix (Quanta Biosciences Beverly, MA #95048–100). Samples were loaded onto a custom design Quant Studio Card using an OpenArray AccuFill System (Life Technologies Carlsbad, CA #4471021) and ran on a QuantStudio 12k Flex Real-Time PCR System (Life Technologies Carlsbad, CA #4471090). Analysis was performed in Expression Suite Software v1.0.4 using *GAPDH* as an internal control. Heatmap was generated using Microsoft Excel software. Select genes highlighting developmental stages towards beta cell differentiation are shown (Fig. 2D).

Histological characterization of pre-implant material occurred by incubating culture aliquots in 4% paraformaldehyde (EMD Chemical Billerica, MA #30525–89-4) solution at 4°C for 24 hours. A 4-hour incubation in a 30% sucrose (Fisher Scientific Waltham, MA #BP220–1) followed. Cellular samples were embedded in O.C.T. (VWR Radnor, PA #25608–930) and frozen on dry ice. Blocks were sectioned on a Leica CM1900 cryostat. Recovered alginate slabs were treated analogously for immunohistochemical preparation. All slides were blocked with 0.1M Tris/HCl (Promega Madison, WI #H5123) pH 7.5 with 0.5% blocking reagent (Perkin Elmer Waltham, MA #FP1012) and 0.1% TrintonX-100 (Fisher Scientific Waltham, MA #BP151) for 1 hour. All antibody solutions were diluted in a 0.1M Tris/HCl pH 7.5 and slides were mounted in a 1:2 dilution of Vectashield mounting medium (Vector Laboratories Burlingame, CA #H-1200). The specific antibodies and the dilutions used are provided in Supp. Table 1. Imaging was performed on an Olympus BX51 microscope using Image Pro Plus software.

Statistical Considerations for the Trial

The Harvard University calculator for power analysis was used during the initial design of the trial (http://hedwig.mgh.harvard.edu/sample_size/js/js_parallel_quant.html). The study was viewed as 2 individual pairwise analyses, in which group 2 and 3 are measured against group 1 (hESCs). To determine the required number of animals per group, we used the following parameters: significance was set at p=0.05, Standard deviation = 2, number of animals = undefined, power = 0.85, difference in means = 4, location of mean in one group as a percentile of the other group = undefined. The power analysis calculation resulted in giving a total of n = 6/group in each paired comparison. The probability was determined to be 87% that the study would detect a treatment difference at a two-sided 0.05 significance level, if the true difference between treatments was 4.000 units.

Results

In vitro characterization of hESC-derived pancreatic progenitors

The directed differentiation of pluripotent stem cells was accomplished as outlined in Fig. 1A. Stage-wise transcript analysis of the differentiating hESC was performed to assay the progression and efficacy of the pancreatic differentiation protocol. An increasingly pancreatic phenotype throughout the protocols different stages was observed (Fig. 1B). The stage 1 induction resulted in a transient expression of *NODAL* and an up-regulation of the definitive endoderm marker *FOXA2. FOXA2* expression was sustained throughout the protocol. The stage 2 through the stage 3 transitions resulted in the up regulations of several pancreatic specific transcripts including *PDX1, HNF1-β, NKX6.1, ONECUT1* and *GLIS3* while stage 4 induced the endocrine related genes *NGN3* and *HEPACAM2,* as well as the endocrine products *GCG, SST,* and *INS.* It should be noted that the relative expression of *SST* was greater than the levels of *GCG* or *INS*. When compared to the human islets, the relative levels of these three endocrine products were low. We conclude that the directed differentiation protocol used resulted in a limited endocrine population.

Previous studies have shown that directed differentiation of pancreatic fates also commonly generates the non-pancreatic endodermal fate of liver and intestines [7,10]. These identities were evaluated through the expression patterns of *HHEX* and *ALB* for liver, and *CDX2* for intestinal development. While low levels of *HHEX* expression was detected throughout the directed differentiation protocol, levels were the highest through stages 3 to stage 4. No significant expression of *ALB* was detected. Together this suggests little to no liver development during the protocol. Likewise low levels of CDX2 expression was detected throughout the early stages of the protocol with a significant level occurring by stage 3 and stage 4, suggesting that portions of the implanted hESC culture had an intestinal, possibly duodenal, characteristic. In addition, the occurrence of mesodermal fates throughout the differentiation event was also noted through the continued expression of the mesodermal markers *MEOX1, THY1* and *COL6A1* (Fig. 1B). We found no strong evidence of other lineages (anterior endoderm, ectoderm) present within the differentiated culture.

To verify these expression patterns we performed an immunohistochemical analysis of the pre-implantation hESC derived cells. Evaluation of the endodermal components of the

culture, as defined by FOXA2 expression, (Fig. 2A–H) demonstrated large FOXA2+ regions co-expressing PDX1 (Fig. 2B–D) implying that the majority of the endodermal cells were of pancreatic identity. In addition, the majority of the FOXA2+ population also co-expressed NKX6.1 (Fig. 2F–H) suggesting a TrPC (trunk- progenitor cell) phenotype; a precursor state to beta cell differentiation. Endocrine differentiation within this culture was scarce, with only small clusters of insulin+ cells present (data not shown). We concluded that group 2 cultures displayed a low percentage of endocrine cells with the majority of the culture expressing characteristics of pancreatic progenitors as defined by the co-expression of FOXA2/PDX1 and FOXA2/NKX6.1.

Macro-encapsulation of the different cellular groups

To understand the feasibility of using the 'βAIR' device in conjunction with these hES-derived cells a rat trial was undertaken (as outlined in Fig. 3A–B (n=17 total)) with the primary end-point being detection of circulating hC-peptide. The majority of the rats quickly recovered from surgeries and lived up to 4 months without any adverse effects. Various rats were put down early in the study to assay the survival and differentiation of the implanted cultures (as indicated in Fig. 3B). Notably very little viable material was recovered from any of the rats in cohort 1 suggesting the environment present in the macroencapsulation device was unfavorable for the survival of undifferentiated hESC. This problem was not observed in cohort 2 or cohort 3 where bio-material was recovered from every rat euthanized.

A typical rat is shown in Fig. 4A. At termination, inspection of the implantation sites/pockets was performed by analyzing tissue immediately adjacent to the device which consistently appeared healthy (Fig. 4B–D). Normally, a vascularized tissue-layer developed at the interface between device and host (Fig. 4B–D). Removal of this associated tissue-layer consistently showed that the alginate slabs and the membrane covering always remained undisrupted (Fig. 4D–E). No indication of any cells breaching the membrane barrier was observed anytime throughout the trial, and in all cases the integrity of the membrane barrier was never compromised.

Encapsulated graft *in vivo* insulin secretion

Since the trial's cellular populations were of human origin, insulin released from implants could be distinguished from endogenous rat insulin. Rats had their blood sampled every other week, and the hC-peptide measurements for fed animals are compiled in Fig. 5A. Considerable variance was detected in hC-peptide levels throughout the trial. For example, group 3 hC-peptide levels during the first week of the trial varied from 70 pM (rat 3–2) to non-detectable levels (rats 3–1 and 3–4) (data used in Fig. 5A).

While non-detectable hC-peptide levels occurred, it should be noted that they did not consistently occur within the same rats from week to week. For example, rat 3–1 had non-detectable hC-peptide levels during the first and third weeks of the trial, but had the highest hC-peptide level detected during the 7^{th} week of the trial (32pM). Overall the average hC-peptide levels in group 3 (human islets) were the highest, and group 1 (undifferentiated hES cells) signals were consistently at the lower limit of detection as would be expected. Finally,

a decreasing level of circulating hC-peptide was noted over the length of the trial for all cohorts.

Two possible reasons for the lowering levels of circulating hC-peptide were explored. First, the possibility that the rats' endogenous β-cell mass was suppressing graft insulin secretion was explored through rendering the rats diabetic via STZ injection. After injection, all of the rats displayed became diabetic, displaying increased blood glucose levels ranging between 18.4 – 28.1mM by 3 days post STZ administration (Supp. Fig. 1A). In addition all rats lost approximately 10% of their body mass during the same time period (Supp. Fig. 1B). Rat blood samples collected on the second and third days post STZ administration did not have increased hC-peptide levels (Supp. Fig. 1C). Rats subsequently had Lin-Plant slow-release insulin pellets subcutaneously placed to assist in control the resulting diabetes. We next explored the possibility that hC-peptide detection in the rat serum was blunted by a host immunological response to the circulating hC-peptide. Serum from insulin-cell bearing rats was assayed for the ability to decrease c-peptide levels in human serum. It was observed that the hC-peptide concentration decreased by as much as 47% (e.g. rat 3–4) indicating the presence of hC-peptide specific antibodies (Fig. 5B).

Explanted devices display widespread expression of endocrine genes

Following euthanasia, devices were recovered for post-implantation ex-vivo function and for histological assessment of graft composition. The recovered post-transplant islets and hES derivatives had a number of functional markers evaluated. Expression of the hormone product C-peptide and the functional marker Urocortin 3 (UCN3) (Fig. 5C–J) were both present and abundant within both cohort 2 and 3. UCN3 expression has previously been shown to coincide with the β-cells ability to respond to changes in glucose concentration [24], and was widely expressed throughout the islet preparation before (not shown) as well as after encapsulation (Fig. 5D). It was noted that UCN3 expression was not limited to β-cells [25]. Widespread UCN3 expression was also noted within the islet-like clusters extracted from the hES-derived group (Fig. 5H & J) and was not restricted to the C-peptide+ regions (Fig. 5J).

We next evaluated the endocrine products on Insulin and Glucagon throughout both cohorts. The recovered human islets were still abundantly producing the hormone products of insulin (Fig. 5K) and glucagon (Fig. 5L), suggestive of the fact that the cells were still at least partially functional. In the case of the hESC-derivatives, smaller islet-like clusters were observed throughout the recovered biomaterial, though at a low percentage (less than 5% of the total culture). Assaying these clusters revealed numerous cells expressing pancreatic endocrine products. While a few poly-hormonal cells were noted, the majority of cells were mono-hormonal expressing only insulin (Fig. 5O) or glucagon (Fig. 5P).

The structural integrity of the recovered islets was further evaluated by investigating if the non-endocrine components were sustained throughout the macroencapsulation event. A major contributing component of islet structure is the capillary networks associated with them. Specifically, we evaluated the expression pattern of von Willebrand Factor (vWF), a plasma protein synthesized within endothelial cells [26], to determine if the capillary network normally associated with islets had been preserved (Fig. 5M). Since the islets were

completely cut off from the rat vasculature, we expected a loss of the endothelial components. However, expression patterns demonstrated at least a partially sustained vasculature within the post-transplantation islets. While this expression pattern does not indicate that the capillary networks retained any functionality, it supports the notion that a higher structural organization within the islet implants was preserved during the macroencapsulation event. When comparing the hESC derived endocrine cluster architecture to that of the human islets no evidence of endothelial cells was found (Fig. 5Q). Altogether, the expression patterns of key functional genes present in the recovered islets are further indicative of a long-term preservation of both the islet architecture and function.

We conclude that ESC-derived cells underwent a limited endocrine cell differentiation in the 'βAIR' device, clustering together into structures resembling pancreatic islets but failing to achieve complete islet architecture and composition.

Discussion

Here we demonstrate that macroencapsulation within the 'βAIR' device can successfully sustain human islets and hESC derivatives within a non-immunosuppressed host. Further, these cellular grafts were found viable four months after initial implantation, demonstrating the possibility for long-term treatment. A particular benefit of this form of macroencapsulation is the negation of safety concerns associated with hESC derivatives (e.g. teratoma risk) because the host is effectively shielded from the implant. Since cells were implanted for an extended period of time, it is clear that no rat immunological components penetrated the membrane barrier. Conversely, there was no indication of human cellular material breaching the device. Previous studies using hESC derivatives as a source of endocrine cells have relied on implanting pancreatic precursors, which in turn differentiate into endocrine sub-types *in vivo*[6,11]. Specifically, in the case of Viacyte, mature endocrine cells cannot be accommodated, as sufficient vascularization occurs several months post-implantation. While our studies used a similar strategy with the majority of the hESC derived cells consisting of pancreatic progenitors, the 'βAIR' technology accommodates fully differentiated endocrine cells, and with current advancements in the ability to generate more mature pluripotent derived endocrine populations in vitro [27,28], future studies should focus on initially encapsulating functional pluripotent derivatives.

When the various cohorts were rendered diabetic via STZ administration none of the implants were capable of sustaining glycemic control. While the present trial was not aimed towards glycemic restoration of a diabetic animal and primarily designed to evaluate the 'βAIR' device's ability to sustain pluripotent derivatives, it is important to note that hC-peptide was detected in serum, though clearly not to the levels needed to sustain homeostasis. A confounding effect of the trial was found to be the development of an immune response to graft-generated hC-peptide which consequently interfered with the ELISA based hC-peptide detection. For that reason, the actual levels of circulating hC-peptide are probably underestimated, and future studies should include cohorts of immunodeficient rats unable to mount an immune response to human proteins. Though the 'βAIR' device is capable of shielding grafts from the host immune system, molecules secreted from the graft into the host circulatory system are not protected from the host's

immune system. With this in mind, future studies combining the 'βAIR' technology with hESC derivatives may benefit from using immune compromised rats to overcome the possibility of an immune response to the grafts secretions.

Additionally, the implanted cell number per device served as a limiting factor. This was guided by the oxygen needs of the human islet preparation and the number of cells implanted per device was matched when using hESC derived cells. It is possible that graft volume of hESC derivatives could be significantly increased since the oxygen demand of pancreatic progenitors are significantly less than the oxygen requirement of islets [29,30,31,32] In addition, the purity of hESC-derived cells was less than absolute, and this may have substantially limited the hESC derived group from the onset of the trial. It is interesting to consider a recent study by Kroon et al [6] in which the authors implanted 2 Encaptra-type sacs both containing between $0.5–1\times10^7$ hESC-derived cells per mouse and compared this to implants of 3000–5000 human islets per mouse. In the current study we implanted ~15–30% of the hESC derived cells and the same number of human islets per rat (an organism app. 10x larger than mice). While not reaching the level of circulating hC-peptide observed in the Kroon et al. study, we did observe circulating hC-peptide within both cohorts throughout the trial. It should also be noted that human islets function poorly in rats [33], and a larger human islet cell mass is generally required for rodent endocrine functions, rendering the rat model a poor host in regard to *in-vivo* functional assessments.

While subject to certain animal model limitations, and constricted by the lack of mature, glucose-responsive insulin producing cells, this study nonetheless demonstrates that cadaveric human islets were successfully sustained within the 'βAIR' device, as were hESC derivatives with a pancreatic phenotype. Immunohistochemical analysis of the human islets recovered after encapsulation further demonstrated that basic islet morphology was preserved and displayed characteristic endocrine markers at similar levels as the starting material. Maturation markers suggest functional endocrine cells were recovered. These data confirm previous finding regarding functional performance of rat islets in a xenogeneic system using the 'βAIR' device [19]

Considering that very little biomaterial was recovered from the Group 1 devices, it is possible that undifferentiated hESCs failed to be sustained in the high oxygen environment of the 'βAIR' device, or alternatively were incapable of maintaining viability given other parameters of the encapsulation event. This latter possibility could be related to forward differentiation and subsequent death, but the study design was not to investigate such events. Because no devices were retrieved at the early time points, we cannot determine between these possibilities. However, the current trial emphasizes that no particular safety concern was identified using pure pluripotent stem cells within the 'βAIR' device and there was no indication of cells breaching the device's membrane barrier. As currently tested, it is unknown if membrane integrity would remain over a period of years, versus months. Long-term deterioration of membrane integrity could eventually compromise the immunoprotective ability and alter the safety profile as well.

In conclusion, the 'βAIR' device technology offers a possible immunoprotective shielding for human endocrine cells, including cells derived from hESC. Additional testing is required

to establish long-term functional retention, and future studies are needed to evaluate hESC derivatives differentiated to a significantly higher functional maturity and purity than those tested in the current trial.

Supplementary Material

Refer to Web version on PubMed Central for supplementary material.

ACKNOWLEDGMENTS

This work was supported by a grant from the Product Development Fund, Cleveland Clinic (J.J). We would like to thank all members of the βAIR/ESC team. In particular we thank the M. Damaser laboratory for technical contributions throughout the trial as well as assisting with the initial surgeries. The UIC islet transplant program is thanked for their assistance during organ acquisition and islet isolation, functional assessments and QC measurements. Special acknowledgements are given to the philanthropic Chicago Diabetes Project (J.O, J.J). We would like to thank OH-Alive for facilitating the QuantStudio analysis of the biological samples, and initial expression analysis. BetaO2 Technologies is thanked for providing expert assistance in handling and implantation of 'βAIR' devices and for general troubleshooting throughout the trial.

J. J. is the guarantor of this work and, as such, had full access to all the data in the study and takes responsibility for the integrity of the data and the accuracy of the data analysis.

Abbreviations:

hESC	human embryonic stem cells
hC-Peptide	human C-Peptide
IP	immunno-precipitation
PTFE	polytetrafluoroethylene
STZ	streptozotocin

References

(1). Qi M; Kinzer K; Danielson KK; Martellotto J; Barbaro B; Wang Y; Bui JT; Gaba RC; Knuttinen G; Garcia-Roca R; Tzvetanov I; Heitman A; Davis M; McGarrigle JJ; Benedetti E; Oberholzer J Five-Year Follow-Up of Patients With Type 1 Diabetes Transplanted With Allogeneic Islets: the UIC Experience. Acta Diabetol. 2014.

(2). Shapiro AM; Lakey JR; Ryan EA; Korbutt GS; Toth E; Warnock GL; Kneteman NM; Rajotte RV Islet Transplantation in Seven Patients With Type 1 Diabetes Mellitus Using a Glucocorticoid-Free Immunosuppressive Regimen. N. Engl. J. Med. 2000, 343, 230–238. [PubMed: 10911004]

(3). Thomson JA; Itskovitz-Eldor J; Shapiro SS; Waknitz MA; Swiergiel JJ; Marshall VS; Jones JM Embryonic Stem Cell Lines Derived From Human Blastocysts. Science 1998, 282, 1145–1147. [PubMed: 9804556]

(4). Fujikawa T; Oh SH; Pi L; Hatch HM; Shupe T; Petersen BE Teratoma Formation Leads to Failure of Treatment for Type I Diabetes Using Embryonic Stem Cell-Derived Insulin-Producing Cells. Am. J. Pathol. 2005, 166, 1781–1791. [PubMed: 15920163]

(5). D'Amour KA; Bang AG; Eliazer S; Kelly OG; Agulnick AD; Smart NG; Moorman MA; Kroon E; Carpenter MK; Baetge EE Production of Pancreatic Hormone-Expressing Endocrine Cells From Human Embryonic Stem Cells. Nat. Biotechnol. 2006, 24, 1392–1401. [PubMed: 17053790]

(6). Kroon E; Martinson LA; Kadoya K; Bang AG; Kelly OG; Eliazer S; Young H; Richardson M; Smart NG; Cunningham J; Agulnick AD; D'Amour KA; Carpenter MK; Baetge EE Pancreatic

Endoderm Derived From Human Embryonic Stem Cells Generates Glucose-Responsive Insulin-Secreting Cells in Vivo. Nat. Biotechnol. 2008, 26, 443–452. [PubMed: 18288110]

(7). Mfopou JK; Chen B; Mateizel I; Sermon K; Bouwens L Noggin, Retinoids, and Fibroblast Growth Factor Regulate Hepatic or Pancreatic Fate of Human Embryonic Stem Cells. Gastroenterology 2010, 138, 2233–45, 2245. [PubMed: 20206178]

(8). Rezania A; Bruin JE; Riedel MJ; Mojibian M; Asadi A; Xu J; Gauvin R; Narayan K; Karanu F; O'Neil JJ; Ao Z; Warnock GL; Kieffer TJ Maturation of Human Embryonic Stem Cell-Derived Pancreatic Progenitors into Functional Islets Capable of Treating Pre-Existing Diabetes in Mice. Diabetes 2012, 61, 2016–2029. [PubMed: 22740171]

(9). Rezania A; Bruin JE; Xu J; Narayan K; Fox JK; O'Neil JJ; Kieffer TJ Enrichment of Human Embryonic Stem Cell-Derived NKX6.1-Expressing Pancreatic Progenitor Cells Accelerates the Maturation of Insulin-Secreting Cells in Vivo. Stem Cells 2013, 31, 2432–2442. [PubMed: 23897760]

(10). Sui L; Geens M; Sermon K; Bouwens L; Mfopou JK Role of BMP Signaling in Pancreatic Progenitor Differentiation From Human Embryonic Stem Cells. Stem Cell Rev. 2013, 9, 569–577.

(11). Schulz TC; Young HY; Agulnick AD; Babin MJ; Baetge EE; Bang AG; Bhoumik A; Cepa I; Cesario RM; Haakmeester C; Kadoya K; Kelly JR; Kerr J; Martinson LA; McLean AB; Moorman MA; Payne JK; Richardson M; Ross KG; Sherrer ES; Song X; Wilson AZ; Brandon EP; Green CE; Kroon EJ; Kelly OG; D'Amour KA; Robins AJ A Scalable System for Production of Functional Pancreatic Progenitors From Human Embryonic Stem Cells. PLoS. One. 2012, 7, e37004.

(12). Hua XF; Wang YW; Tang YX; Yu SQ; Jin SH; Meng XM; Li HF; Liu FJ; Sun Q; Wang HY; Li JY Pancreatic Insulin-Producing Cells Differentiated From Human Embryonic Stem Cells Correct Hyperglycemia in SCID/NOD Mice, an Animal Model of Diabetes. PLoS. One. 2014, 9, e102198.

(13). Kirk K; Hao E; Lahmy R; Itkin-Ansari P Human Embryonic Stem Cell Derived Islet Progenitors Mature Inside an Encapsulation Device Without Evidence of Increased Biomass or Cell Escape. Stem Cell Res. 2014, 12, 807–814. [PubMed: 24788136]

(14). Richardson T; Kumta PN; Banerjee I Alginate Encapsulation of Human Embryonic Stem Cells to Enhance Directed Differentiation to Pancreatic Islet-Like Cells. Tissue Eng Part A 2014.

(15). Colton CK Oxygen Supply to Encapsulated Therapeutic Cells. Adv. Drug Deliv. Rev. 2014, 67-68, 93–110. [PubMed: 24582600]

(16). Ludwig B; Zimerman B; Steffen A; Yavriants K; Azarov D; Reichel A; Vardi P; German T; Shabtay N; Rotem A; Evron Y; Neufeld T; Mimon S; Ludwig S; Brendel MD; Bornstein SR; Barkai U A Novel Device for Islet Transplantation Providing Immune Protection and Oxygen Supply. Horm. Metab Res. 2010, 42, 918–922. [PubMed: 21031332]

(17). Ludwig B; Reichel A; Steffen A; Zimerman B; Schally AV; Block NL; Colton CK; Ludwig S; Kersting S; Bonifacio E; Solimena M; Gendler Z; Rotem A; Barkai U; Bornstein SR Transplantation of Human Islets Without Immunosuppression. Proc. Natl. Acad. Sci. U. S. A 2013, 110, 19054–19058. [PubMed: 24167261]

(18). Barkai U; Weir GC; Colton CK; Ludwig B; Bornstein SR; Brendel MD; Neufeld T; Bremer C; Leon A; Evron Y; Yavriyants K; Azarov D; Zimermann B; Maimon S; Shabtay N; Balyura M; Rozenshtein T; Vardi P; Bloch K; de VP; Rotem A Enhanced Oxygen Supply Improves Islet Viability in a New Bioartificial Pancreas. Cell Transplant. 2013, 22, 1463–1476. [PubMed: 23043896]

(19). Neufeld T; Ludwig B; Barkai U; Weir GC; Colton CK; Evron Y; Balyura M; Yavriyants K; Zimermann B; Azarov D; Maimon S; Shabtay N; Rozenshtein T; Lorber D; Steffen A; Willenz U; Bloch K; Vardi P; Taube R; de VP; Lewis EC; Bornstein SR; Rotem A The Efficacy of an Immunoisolating Membrane System for Islet Xenotransplantation in Minipigs. PLoS. One. 2013, 8, e70150.

(20). Ludwig B; Rotem A; Schmid J; Weir GC; Colton CK; Brendel MD; Neufeld T; Block NL; Yavriyants K; Steffen A; Ludwig S; Chavakis T; Reichel A; Azarov D; Zimermann B; Maimon S; Balyura M; Rozenshtein T; Shabtay N; Vardi P; Bloch K; de VP; Schally AV; Bornstein SR; Barkai U Improvement of Islet Function in a Bioartificial Pancreas by Enhanced Oxygen Supply

and Growth Hormone Releasing Hormone Agonist. Proc. Natl. Acad. Sci. U. S. A 2012, 109, 5022–5027. [PubMed: 22393012]

(21). Gangemi A; Salehi P; Hatipoglu B; Martellotto J; Barbaro B; Kuechle JB; Qi M; Wang Y; Pallan P; Owens C; Bui J; West D; Kaplan B; Benedetti E; Oberholzer J Islet Transplantation for Brittle Type 1 Diabetes: the UIC Protocol. Am. J. Transplant. 2008, 8, 1250–1261. [PubMed: 18444920]

(22). Ricordi C; Lacy PE; Finke EH; Olack BJ; Scharp DW Automated Method for Isolation of Human Pancreatic Islets. Diabetes 1988, 37, 413–420. [PubMed: 3288530]

(23). Barbaro B; Salehi P; Wang Y; Qi M; Gangemi A; Kuechle J; Hansen MA; Romagnoli T; Avila J; Benedetti E; Mage R; Oberholzer J Improved Human Pancreatic Islet Purification With the Refined UIC-UB Density Gradient. Transplantation 2007, 84, 1200–1203. [PubMed: 17998877]

(24). Blum B; Hrvatin SS; Schuetz C; Bonal C; Rezania A; Melton DA Functional Beta-Cell Maturation Is Marked by an Increased Glucose Threshold and by Expression of Urocortin 3. Nat. Biotechnol. 2012, 30, 261–264. [PubMed: 22371083]

(25). van der Meulen T; Xie R; Kelly OG; Vale WW; Sander M; Huising MO Urocortin 3 Marks Mature Human Primary and Embryonic Stem Cell-Derived Pancreatic Alpha and Beta Cells. PLoS. One. 2012, 7, e52181.

(26). Bellacen K; Kalay N; Ozeri E; Shahaf G; Lewis EC Revascularization of Pancreatic Islet Allografts Is Enhanced by Alpha-1-Antitrypsin Under Anti-Inflammatory Conditions. Cell Transplant. 2013, 22, 2119–2133. [PubMed: 23050776]

(27). Pagliuca FW; Millman JR; Gurtler M; Segel M; Van DA; Ryu JH; Peterson QP; Greiner D; Melton DA Generation of Functional Human Pancreatic Beta Cells in Vitro. Cell 2014, 159, 428–439. [PubMed: 25303535]

(28). Rezania A; Bruin JE; Arora P; Rubin A; Batushansky I; Asadi A; O'Dwyer S; Quiskamp N; Mojibian M; Albrecht T; Yang YH; Johnson JD; Kieffer TJ Reversal of Diabetes With Insulin-Producing Cells Derived in Vitro From Human Pluripotent Stem Cells. Nat. Biotechnol. 2014, 32, 1121–1133. [PubMed: 25211370]

(29). Cechin S; Alvarez-Cubela S; Giraldo JA; Molano RD; Villate S; Ricordi C; Pileggi A; Inverardi L; Fraker CA; Dominguez-Bendala J Influence of in Vitro and in Vivo Oxygen Modulation on Beta Cell Differentiation From Human Embryonic Stem Cells. Stem Cells Transl. Med. 2014, 3, 277–289. [PubMed: 24375542]

(30). Fraker CA; Alvarez S; Papadopoulos P; Giraldo J; Gu W; Ricordi C; Inverardi L; Dominguez-Bendala J Enhanced Oxygenation Promotes Beta-Cell Differentiation in Vitro. Stem Cells 2007, 25, 3155–3164. [PubMed: 17761759]

(31). Fraker CA; Ricordi C; Inverardi L; Dominguez-Bendala J Oxygen: a Master Regulator of Pancreatic Development? Biol. Cell 2009, 101, 431–440. [PubMed: 19583566]

(32). Heinis M; Simon MT; Ilc K; Mazure NM; Pouyssegur J; Scharfmann R; Duvillie B Oxygen Tension Regulates Pancreatic Beta-Cell Differentiation Through Hypoxia-Inducible Factor 1alpha. Diabetes 2010, 59, 662–669. [PubMed: 20009089]

(33). Pepper AR; Gall C; Mazzuca DM; Melling CW; White DJ Diabetic Rats and Mice Are Resistant to Porcine and Human Insulin: Flawed Experimental Models for Testing Islet Xenografts. Xenotransplantation. 2009, 16, 502–510. [PubMed: 20042050]

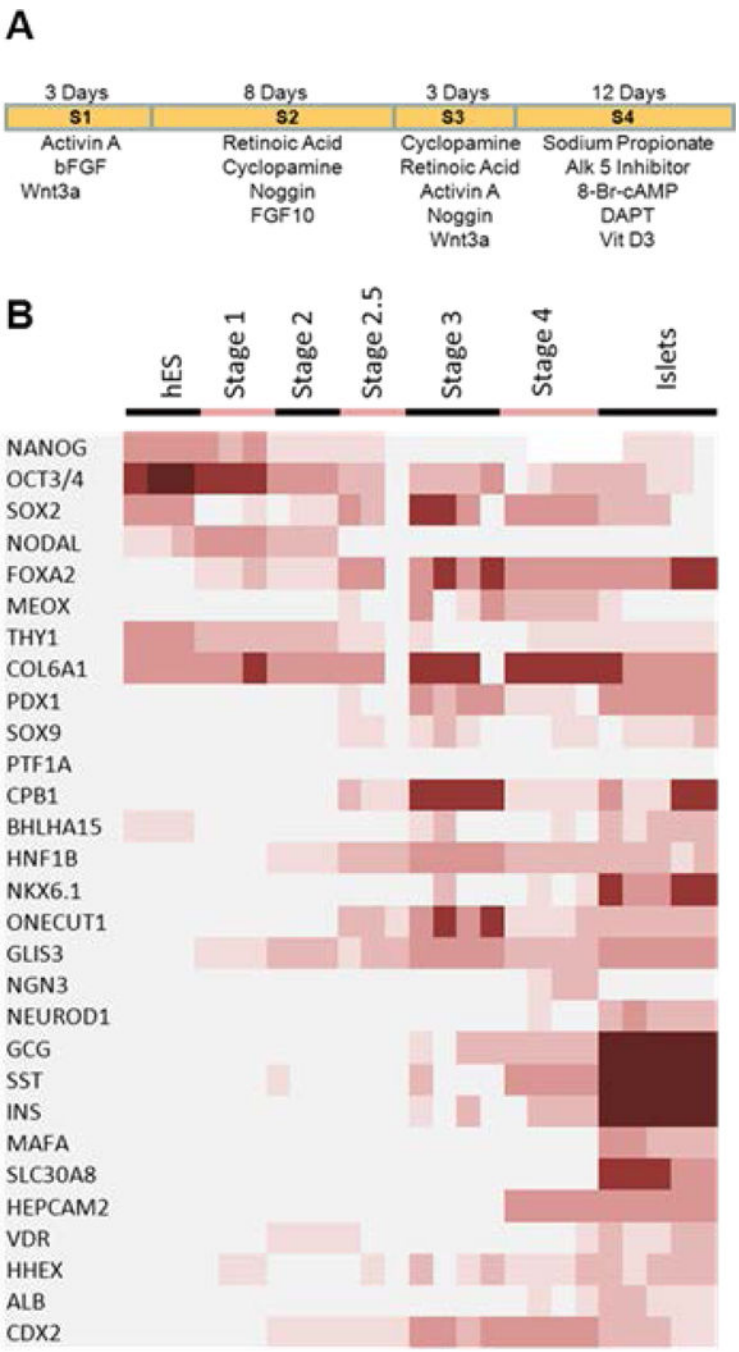

Figure 1 –. Directed differentiation of hES cells toward pancreatic fates.

Panel A shows the directed differentiation protocol used to generate the hES derivatives used throughout the trial. Panel B shows a heat map of selected genes assayed at the different stages of the directed differentiation protocol as compared to the expression pattern of human islets.

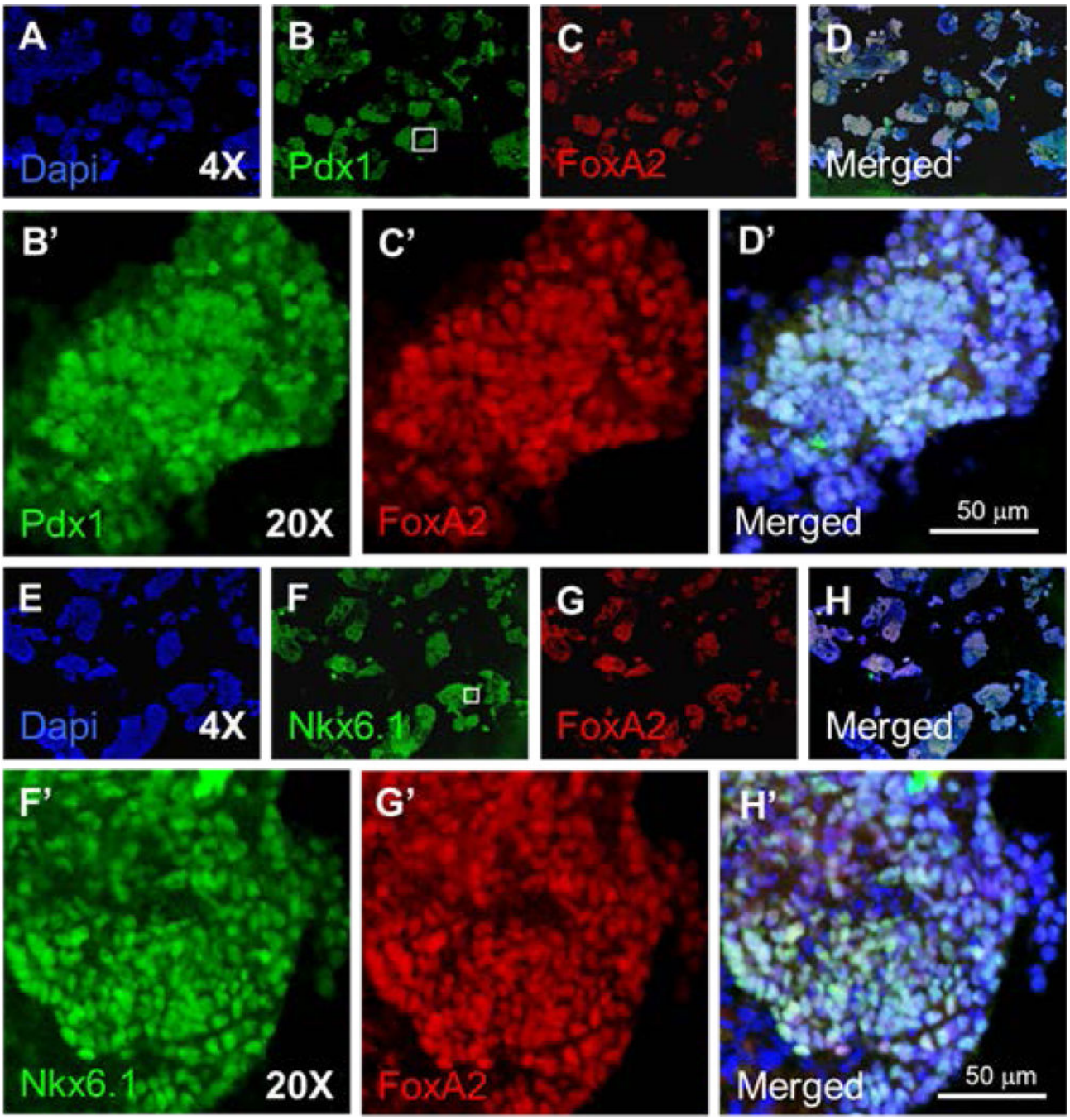

Figure 2 –. IHC analysis of preimplantation hESC derivatives.

Panels A-D were stained for the pancreatic progenitor marker PDX1 (Panel B) and the endodermal marker FOXA2 (Panel C). Panels E-H were stained for the TrPC marker Nkx6.1 (Panel F) and the endodermal marker FoxA2 (Panel G). Prime letters are higher magnification images from the region indicated by the box in panel B & F.

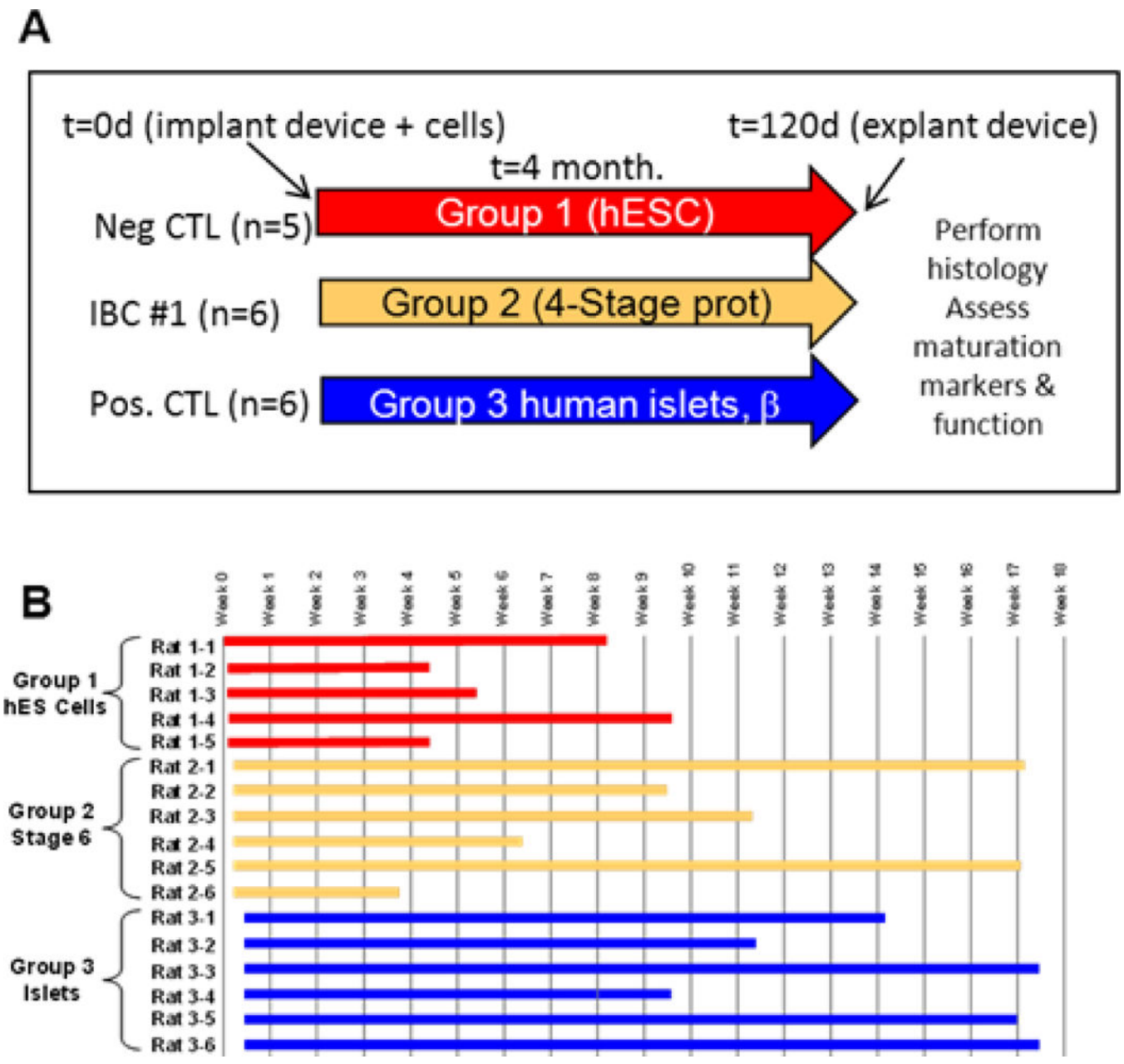

Figure 3 –. Schematic outline of trial.

Panel A shows a schematic of the three different trial cohorts. Implanted devices were loaded with cells as follows; Group 1 was loaded with pluripotent hESC, Group 2 was loaded with hESC differentiated into pancreatic precursors with limited endocrine fate conversion using a 4-stage protocol, Group 3 was loaded with human islet preparations. Panel B shows a timeline for each rat in the trial.

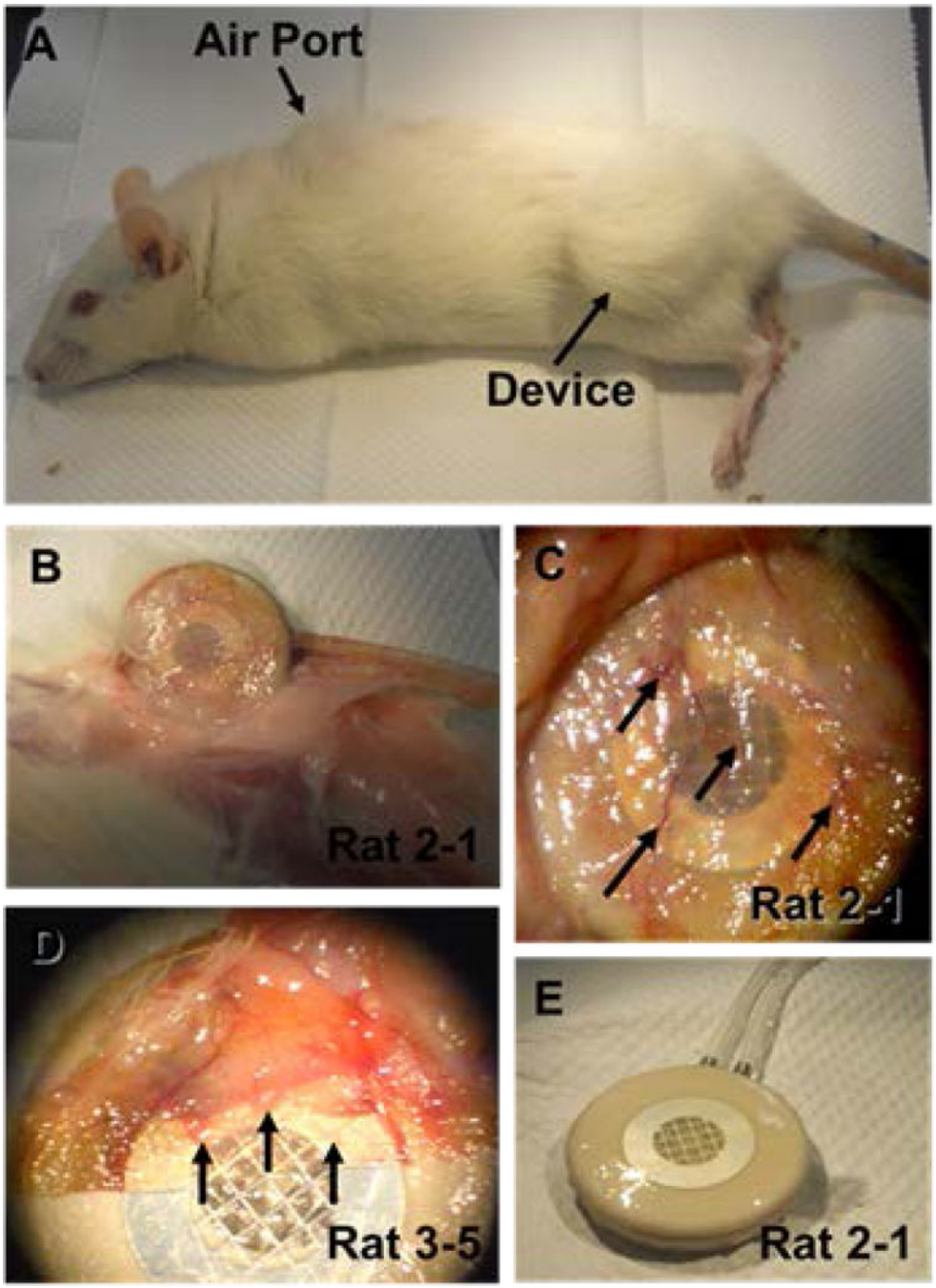

Figure 4 –. Explantation of macro-encapsulation device.

Panel A shows a typical rat after euthanasia. Arrow heads denote the subcutaneous positioning of the device and the air ports. Panel B and C show the recovery of the macro-encapsulation device from rat 2-1 and the tissue layer associated with it. Panel D shows the recovered device from rat 3-5 with the associated tissue layer partial pulled back. Arrows in panels C-D show vessels that are present in this tissue covering. Panel E shows the device recovered from rat 2-1 after the associated tissue layer was removed from it.

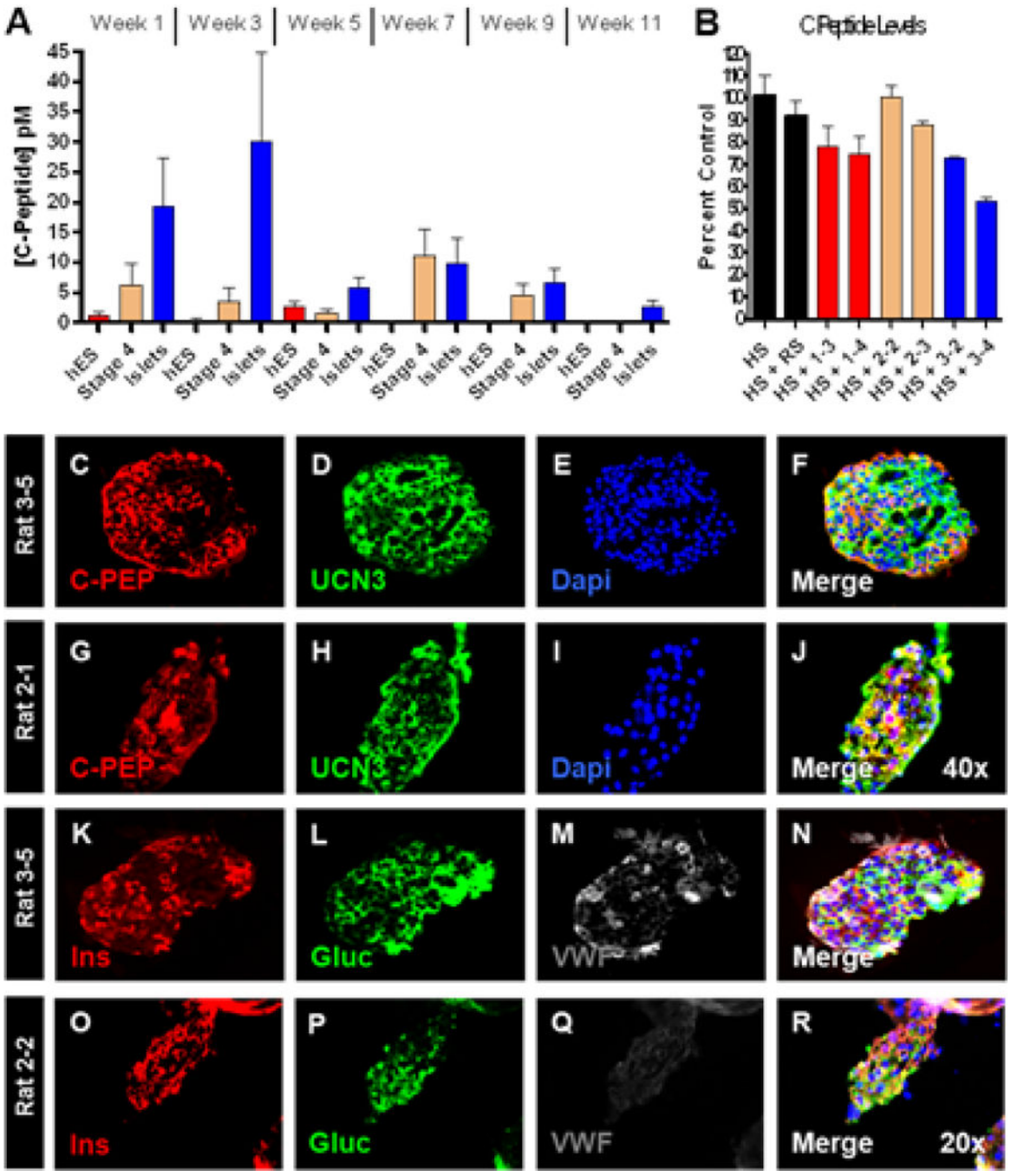

Figure 5 –. In trial measurements and post-trial recovery.

Panel A shows the average biweekly serum hC-peptide concentration per group for the length of the trial. Panel B shows the depletion of C-peptide from human serum by serum from representative rats from the trial indicated on the x-axis. Abbreviations are as follows: human serum (HS), control rat serum (RS) and numbers are rat serum recovered from the indicated cohorts (ie 1–3 is rat 3 from group 1). Panels C-J show immunofluorescence staining for C-Peptide and Urocortin-3 on recovered islets (panels C-F) and hESC derivatives (panels G-J). Panels K-R show immunofluorescence staining for Insulin,

Glucagon and Von Willebrand Factor on recovered islets (panels K-N) and hESC derivatives (panels O-R).